

The methane mussel: roles of symbiont and host in the metabolic utilization of methane

R. E. Kochevar¹, J. J. Childress¹, C. R. Fisher², and E. Minnich³

¹ Department of Biological Sciences and Marine Science Institute, University of California, Santa Barbara, California 93106, USA

² Department of Biology, 208 Mueller Laboratory, Pennsylvania State University, University Park, Pennsylvania 16801, USA

³ Panlabs, 11804 North Creek Parkway South, Bothel, Washington 98011-8805, USA

Date of final manuscript acceptance: November 8, 1991. Communicated by M. G. Hadfield, Honolulu

Abstract. Methane mussels (*Bathymodiolus* sp., undescribed; personal communication by R. Turner to CRF) were collected in September 1989 and April 1990 from offshore Louisiana in the Gulf of Mexico. These mussels contain endosymbiotic methane-oxidizing bacteria and are capable of utilizing environmental methane as a source of energy and carbon. Oxygen consumption, methane consumption, and carbon dioxide production were measured in mussels with intact symbionts, functionally aposymbiotic mussels, and separated symbiont preparations under controlled oxygen and methane conditions, in order to study the roles of the symbionts and the hosts in methane utilization. The association was found to be very efficient in fixing methane carbon (only ~30% of CH₄ consumed is released as CO₂), and to be capable of maximal rates of net carbon uptake of nearly 5 μmol g⁻¹ h⁻¹. Rates of oxygen and methane consumption were dependent upon oxygen and methane concentrations. Maximal consumption rates were measured at 250 to 300 μM O₂ and 200 to 300 μM CH₄, under which conditions, oxygen consumption by the gill tissues (containing symbionts) had increased more than 50-fold over rates measured in the absence of methane. A model is proposed for the functioning of the intact association in situ, which shows the symbiosis to be capable of achieving growth rates (net carbon assimilation) in the range of 0.003 to 0.50% per day depending upon oxygen and methane concentrations. Under the conditions measured in the seep environment (200 μM O₂, 60 μM CH₄), a mussel consuming methane at rates found to be typical (4 to 5 μmol g⁻¹ h⁻¹) should have a net carbon assimilation rate of about 0.1% per day. We suggest that the effectiveness of this symbiosis arises through integration of the morphological and physiological characteristics inherent to each of the symbiotic partners, rather than from extensive specialization exhibited by other deep-sea chemotrophic associations.

Introduction

The existence of symbiotic associations between invertebrates and chemotrophic bacteria has been recognized since 1980 (Cavanaugh et al. 1981, Felbeck et al. 1981). We now know that host animals are taxonomically diverse, with representatives from at least six invertebrate phyla (Fisher 1990), and that these symbioses occur in a wide variety of habitats, ranging from regions of tectonic activity such as deep-sea hydrothermal vents and subduction zones, to areas characterized by human impact such as sewage outfall and paper-mill effluent sites (Somero et al. 1989, Fisher 1990). The vast majority of the chemotrophic symbioses described thus far rely upon reduced sulfur as a source of chemical energy. However, the existence of symbioses capable of utilizing other reduced chemical compounds such as hydrogen, iron, ammonia, or methane, has been considered a possibility since the initial discovery of the hydrothermal vents.

The "methane mussel" symbiosis of the Louisiana slope (*Bathymodiolus* sp., undescribed) inhabits regions of the continental margin where natural gas, composed primarily of methane, seeps through the sediments to the oxygenated benthic water (MacDonald et al. 1989), and is one of a few symbioses in which the ability to utilize methane has been unequivocally demonstrated (Childress et al. 1986, Fisher et al. 1987, Schmaljohann and Flügel 1987, Fisher 1990). Morphologically, it is similar to the hydrothermal vent mussel *B. thermophilus*, having a somewhat reduced digestive tract and enlarged, fleshy gills. Transmission electron micrographs of these gills have shown them to contain abundant intracellular bacteria with stacked membrane structures characteristic of Type I methanotrophs (Childress et al. 1986, Fisher et al. 1987). Measurements of respiration by intact mussels and by excised gills showed that, under aerobic conditions, oxygen and methane were consumed at high rates, and that CO₂ production increased during methane consumption, indicating oxidation of methane (Childress et al. 1986). Methane oxidation was further demonstrated by incubating excised gills with radiolabeled methane.

After 3 h, ~50% of the radioactive methane consumed had been incorporated into the gill tissue as ^{14}C -organic compounds and the rest had been oxidized to $^{14}\text{CO}_2$ (Fisher et al. 1987).

Additional evidence for the importance of methanotrophy in this symbiosis has been provided by stable carbon-isotope studies. $\delta^{13}\text{C}$ values of both gill and mantle tissue samples are very light ($\delta^{13}\text{C} = -57.6$ to -40.1 per mil), and are closely correlated with the stable isotopic composition of the methane source where the samples were collected (Childress et al. 1986, Brooks et al. 1987). This implies that in situ, methane from the seeps serves as the primary carbon source for the mussels as well as the bacterial endosymbionts. Shell growth with methane as the sole carbon and energy source has also been demonstrated for this species by Cary et al. (1988).

This study was designed to provide a quantitative description of the relationships between oxygen consumption, methane consumption, and carbon dioxide production in this symbiosis, and to explore the effects of oxygen and methane concentrations on these rates. By measuring the consumption and production rates of these metabolic gases in whole mussels and symbiont preparations under a variety of dissolved gas conditions, we were able to examine the effects of variation in environmental concentrations upon the metabolism of the intact symbiosis, as well as gain insight into the nature of interaction between symbiont and host.

Materials and methods

Mussel collection

Bathymodiolus sp. (undescribed)¹ was collected in the Gulf of Mexico from the Green Canyon offshore leasing area, Blocks 184 and 185 (27°41'N, 91°32'W; 210 km south-southwest of Grand Isle, Louisiana, USA). The mussels were recovered from depths between 600 and 700 m, using the research submersibles "Pisces II" in September 1989 and "Johnson Sea Link I" in April 1990. The mussels were gathered with the manipulator arm of the submersible and placed in a thermally-insulated basket for transport to the surface.

Mussel maintenance

Upon reaching the surface, the mussels were transferred to containers of chilled seawater kept in a refrigerated chest (~7°C). Water in these containers was changed daily, and bubbled twice daily with methane and air for 10 min per container. For transport, the mussels were placed in 4-liter polypropylene jars filled with chilled, air- and methane-bubbled seawater. These jars were then packed in ice chests and air-freighted to Santa Barbara, California.

In the laboratory, the mussels were housed in plastic cages submerged in a 1400-liter, flowing seawater tank held at 7 to 8°C in a walk-in cold room. The water in the holding tank was continuously

bubbled with air and natural gas comprised primarily of methane (Southern California Gas Company).

One group of mussels was exposed to seawater at elevated temperature (~11°C) for a period of about 24 h. Subsequent respiration experiments carried out at 7 to 8°C revealed that these individuals did not consume methane at measurable rates ($<0.1 \mu\text{mol g}^{-1} \text{hg}^{-1}$), and were therefore considered to be functionally aposymbiotic. These mussels were used as controls in several experiments.

Transmission electron microscopy (TEM)

Gill filaments were removed from a freshly-collected and a functionally aposymbiotic mussel gill and immediately fixed in 3% glutaraldehyde in 0.1 M phosphate-buffered 0.35 M sucrose, pH 7.3 (PBS). This tissue was stored in fixative for up to 2 wk at 4°C, after which it was washed in PBS and postfixed in 1% osmium tetroxide for 1 h (Fisher et al. 1987). Tissue from the freshly-collected mussel was dehydrated through a graded ethanol series, while that from the functionally aposymbiotic mussel was dehydrated by a 10 min immersion in acidified 2,2-dimethoxypropane, followed by 3 to 10 min washes in propylene oxide (Muller and Jacks 1975). Following dehydration, individual gill filaments were embedded in Spurr's embedding medium. Thin sections were cut using a Sorvall MT2 microtome, stained with uranyl acetate and lead citrate, and examined on a JEOL 1200 EX2 electron microscope.

Bacterial counts

To determine the relative numbers of bacteria in gills from a freshly collected mussel, a mussel maintained in captivity for 26 d, and a functionally aposymbiotic mussel, frozen samples of gill tissue were thawed and subsequently lightly ground in 10% formaldehyde in artificial seawater using a ground-glass tissue grinder. After appropriate dilution, aliquots of the homogenates were stained with 1 mg/l 4',6-diamidino-2-phenylindole (DAPI) for 5 min and collected on a black, 0.2 μm Nucleopore filter (Hobbie et al. 1977). Densities of bacteria were determined by epifluorescence counting of fluorescing bodies of appropriate size (~1 μm), at seven different locations on each filter. Two separate homogenates were prepared from each mussel.

Flow-through pressure respirometry

Seawater was first passed through a 5.0 μm filter, sterilized by ultraviolet-light, and then filtered through 5.0 and 0.2 μm filters. This sterilized seawater, along with penicillin-G solution (final concentration 80 mg l^{-1}), was then pumped into a water/gas mixing column.

The water/gas mixing column (Fig. 1) consisted of a 1 m length of 3" nominal (7.65 cm i.d.) diameter polyvinyl chloride (PVC) tube, capped at both ends, fitted with various fluid inlet/outlet and probe ports. It was designed to maintain constant water level, pH, and pressure through the use of a water level controller (Levelite), a pH controller (ProMinent), and a back-pressure relief valve (Ryan Herco). The bottom cap of the column housed aquarium air stones through which oxygen, methane and nitrogen were bubbled to achieve desired concentrations.

Seawater from the column was pumped at a constant flow rate (usually 5 or 8 ml min^{-1} , depending upon the size of the experimental mussels) and pressure (80 psi) to the three respiration chambers (two experimental and one control), via three chemical metering pumps (Crane). The chambers (Fig. 2) consisted of acrylic tubes (33 cm length; 10 cm o.d.; 2.56, 5.13, or 7.69 cm i.d., matched) with "O" ring-sealed Hastelloy-C top and bottom caps, placed in snug-fitting stainless steel sleeves housing remote-control electromagnetic stirrers (Cole-Parmer) in their bases. The top cap of each chamber contained fittings for two 16" nominal (~0.76 mm i.d.) Hastelloy-C

¹ Although the methane mussel studied here is referred to throughout as *Bathymodiolus* sp., the process of description was not complete at the time of writing. It was now temporarily designated as Seep Mytilid Ia, to distinguish it from among several similar species found in the Gulf of Mexico (personal communication from R. Gustafson to REK). R. Gustafson also noted that it is premature to refer to the seep mytilids as belonging to the genus *Bathymodiolus* or to the subfamily Bathymodiolinae

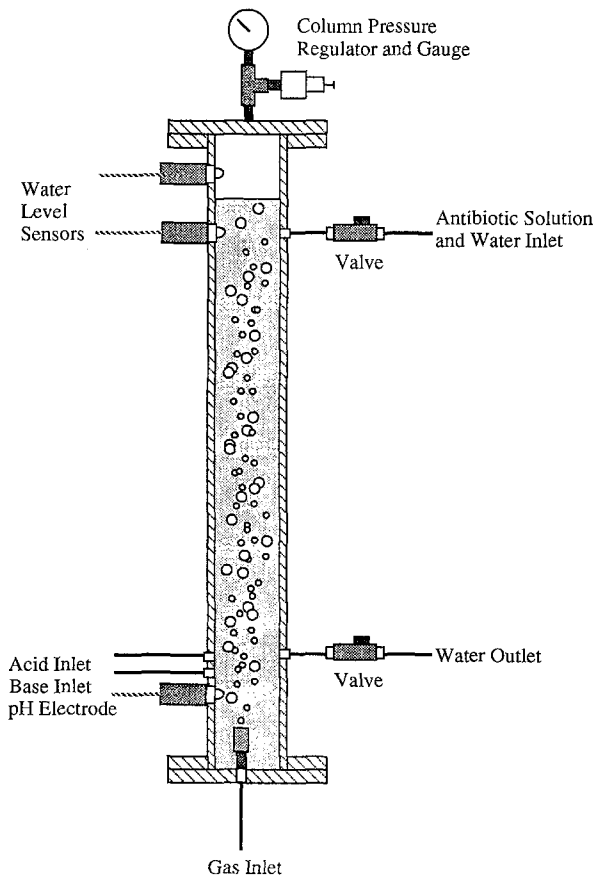


Fig. 1. Water/gas mixing column used to control dissolved gas concentrations and pH of water entering respirometer. Filtered seawater and antibiotic solutions entered through inlet, were bubbled continuously with oxygen, methane, and nitrogen from air stones in column base, and exited *via* outlet to respiration chambers

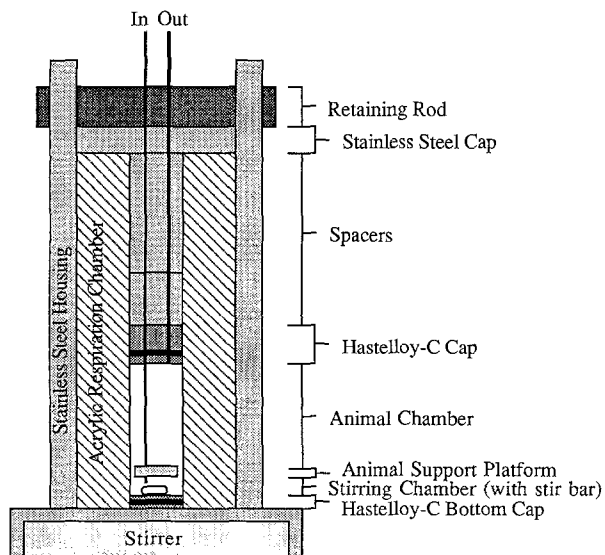


Fig. 2. Cutaway diagram of high-pressure respiration chamber in which mussels (*Bathymodiolus* sp.) were placed for experimentation. Mussels rested upon animal-support platform, which is perforated, and seawater from column entered through inlet tube, mixed, and exited through exit tube for analysis. Entire chamber was submerged in temperature-controlled water bath

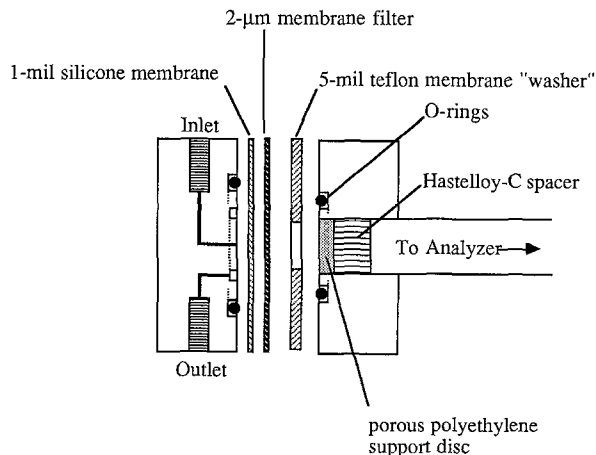


Fig. 3. Cutaway diagram of membrane inlet mass spectrometry (MIMS) interface port. Acidified seawater to be analyzed passed over gas-permeable silicone membrane, through which dissolved gases diffused. These gases then entered vacuum chamber for analysis by mass spectrometer

tubes: an inflow tube, run to the bottom of the chamber, and an exit tube, mounted flush with the bottom of the cap. On the bottom of each vessel was a teflon-coated stir bar, above which the mussel rested on a perforated acrylic platform attached to the inflow tube. The respiration chambers were immersed in a water-filled reservoir, held at a constant temperature (6.0°C) by a recirculating water bath.

As the seawater exited the chambers, it was passed through automatically-actuated stream-switching valves and analyzed by one of two methods.

For gas chromatographic analysis, the effluent seawater was automatically sampled at 20 to 30 min intervals, acidified and heated in a stirring chamber, and injected on a Hewlett-Packard 5880 A gas chromatograph (GC), modified for automatic sampling and analysis of water samples (Childress et al. 1984, Anderson et al. 1987). The GC analyzed the concentrations (μM) of CO_2 , O_2 , N_2 , and CH_4 in the effluent chamber water, alternating between the control and the experimental streams every three injections.

The other method of analysis utilized a membrane-inlet mass spectrometer (MIMS), with a small quadrupole analyzer (Hiden Analytical Ltd.) attached to a Macintosh II computer programmed for automatic sample-stream switching, data acquisition, and data analysis. In this method, effluent water was mixed with argon-bubbled 50% phosphoric acid (to convert all dissolved carbonates to CO_2), heated to 70°C, and passed over a gas-permeable 1 mil nominal (27.8 μm) silicone membrane (MEM-213 from General Electric), backed with a 2 μm pore filter (Nuclepore) and a 5 mil nominal (139 μm) teflon "washer" (Fralock), supported by a disc of 10 μm -pore porous polyethylene (Porex Technologies; Fig. 3).

As water passed over the membrane, gases in solution diffused into the vacuum chamber, allowing the dissolved gas composition of the sample stream to be analyzed. Heinze et al. (1983) give a complete description of this process. For each analysis, the partial pressures of CO_2 (monitored at 44 atomic mass units, amu), O_2 (32 amu), N_2 (28 amu), CH_4 (monitored at 15 amu to avoid the O_2 daughter peak at 16 amu), and Ar (40 amu, used as an indicator of sample and acid flow rates) present within the vacuum chamber were measured in sequence. These partial-pressure measurements were then converted to units of μmol dissolved gas l^{-1} (using conversion factors based on periodic GC injections from the sample stream), averaged until 100 such analyses had been completed, and stored on computer diskette. This entire process took approximately 10 min, after which the sample stream was automatically switches, the analytical system allowed to come to steady state with the new sample stream for about 4 min, and the process then repeated.

Because both methods of analysis involved acidification of the seawater samples, the term "CO₂" will be used to refer to the concentrations of CO₂ measured by each analytical process, regardless of the specific chemical species present in the seawater samples prior to acidification (e.g. H₂CO₃, HCO₃⁻, etc.).

Experimental procedure for whole-mussel experiments

At the beginning of each experiment, the mussels' valves were scrubbed clean of visible contaminating material and rinsed in chilled seawater. The mussels were then lowered into the respiration chambers and incubated in the presence of oxygen ([O₂] > 100 μM) and methane ([CH₄] > 60 μM) until their valves opened and metabolic gas concentrations remained consistent through several analyses from each chamber, a condition hereafter referred to as "steady state". Once steady state conditions had been established and maintained for a sufficient period of time to make several analyses from each chamber (usually 10 to 12 h with the GC, or 1 to 2 h with the MIMS), the gas concentrations were changed. In this fashion, the gas consumption or production rates for each individual were measured at different concentrations of oxygen and methane. Upon termination of an experiment (usually after 72 to 96 h), the mussels were removed from the chambers and dissected. The following measurements were taken: Shell length, drained weight, gill weight, and total shell-free wet-tissue weight.

To determine the consumption or production rates of dissolved gases, the average of each set of analyses from the experimental chamber was compared to the average of the sets of analyses from the control chamber immediately preceding and following the experimental set. Using the flow rate through the chamber and the wet weight of the mussel, these differences in gas concentrations were converted to mass-specific gas production or consumption values in μmol g (shell-free wet tissue wt)⁻¹ h⁻¹ (abbreviated μmol g⁻¹ h⁻¹).

Experimental procedure for symbiont preparation experiments

All these experiments were conducted at sea with tissue from freshly recovered mussels. For each of the two symbiont preparation experiments ("S1" and "S2"), bacterial suspensions were prepared by homogenizing about 3 g of gill tissue for 30 s in a ground-glass tissue homogenizer in an approximately 10 × volume of imidazole bacterial isolation buffer (Distel and Felbeck 1988). The resulting homogenate was squeezed by hand through 100 μm Nitex screen, loaded into a syringe, and sequentially filtered through 50, 25, and 10 μm-mesh Nitex screens and a 5 μm Nuclepore filter. The cells which passed through the filters were washed twice by pelleting them in a table-top centrifuge (at about 2800 rpm) and resuspended in 0.2 μm filtered seawater to a final volume of 5.0 ml. This entire procedure was conducted in a cold room (~7°C) and took less than 15 min.

Of the bacterial suspension, 100 μm aliquots were placed in individual 28 ml serum vials with 10 ml of 0.2 μm-filtered seawater. The head space of each vial was purged for 30 s with N₂ gas, then the vial was sealed with a split grey-butyl rubber stopper and capped. From each vial, 8.55 ml of N₂ was removed and replaced with air to achieve a dissolved O₂ concentration of 100 μM. Methane was added to the head space to achieve desired dissolved methane concentrations, and the vials were shaken for 60 s to equilibrate the gases with the seawater.

After 30 min, ¹⁴C-methane was added to each vial to achieve final activities between 0.13 and 4.41 μCi μmol⁻¹, depending upon the experiment and the total methane concentration. Final ¹⁴CH₄ activities were calculated based upon total [CH₄] and known activities of ¹⁴CH₄ stock added. The vials were then shaken for 1 min to begin the experiments. The contents of the vials were fixed in triplicate for each methane concentration every 20 min for 1 h. This

resulted in a total of nine experimental vials per methane concentration studied, not including controls. Fixation was achieved at each time point by addition of 600 μl of a mixture of formalin and 10N NaOH (5:1) to each of three vials. This killed the bacteria and scrubbed the head space of CO₂. As controls, 0.5 ml of formalin was initially added to one vial at each methane concentration and allowed to incubate for the full hour.

One hour after all incubations had been fixed, each vial was opened and samples of the bacterial suspension were removed from two of the three replicates from each time point, evaporated to dryness, and transported back to the laboratory. The vials were then capped with stoppers from which were suspended filters containing 100 μl of phenylethylamine. After sealing, the vials were acidified with 100 μl of 16N H₂SO₄ and allowed to sit over night. During this step, the HCO₃⁻ in the seawater and tissue was converted to CO₂ and adsorbed onto the filters as it diffused into the head space. The following morning, the filters were transferred to scintillation vials containing 100 μl of 20% methanol to keep them moist, and sealed with caps and Parafilm for the return trip to the laboratory. Controls run to estimate loss of phenylethylamine-trapped CO₂ during methanol storage and transport have shown less than 2% loss over 12 d period.

Upon returning to the laboratory, the bacterial suspension samples were digested in 600 μl of a quaternary amine (TS-1 from National Diagnostics) and neutralized before addition of fluor (3a70 from Research Products International). All samples were counted on a Beckman LS 6800 liquid scintillation counter for 5 min, and corrections were made for background, efficiency, and quenching using the "H#" method. Densities of bacteria in the bacterial suspensions were determined in the manner described in the "Bacterial counts" subsection above, using epifluorescence counting of aliquots of the original bacterial suspension fixed at sea in 3% glutaraldehyde in PBS.

Statistical analysis and presentation of the data

Linear regressions and other simple statistics were done using Statview II (Abacus Concepts). Analyses of covariance were performed using Super ANOVA (Abacus Concepts).

Results

Electron microscopy and bacterial counts

Electron micrographs of gill tissue from a freshly-collected mussel (*Bathymodiolus* sp. undescribed) and a functionally aposymbiotic mussel indicate the presence of degenerate bacteria in functionally aposymbiotic gill tissue, of the appropriate size for DAPI (4',6-diamidino-2-phenylindole) counting. However, no bacteria were found which contained the stacked-membrane structures present in "healthy" symbionts from freshly-collected mussel gills (Fig. 4; and Childress et al. 1986, Fisher et al. 1987).

The DAPI-stained bodies present in the functionally aposymbiotic tissue homogenate were not as regular in shape as those counted in the other two samples. Counts of DAPI-stained gill homogenates from a freshly-collected mussel, a mussel maintained in captivity for 26 d, and a functionally aposymbiotic mussel showed substantially reduced densities (to ~10%) in the functionally aposymbiotic individual (Table 1).

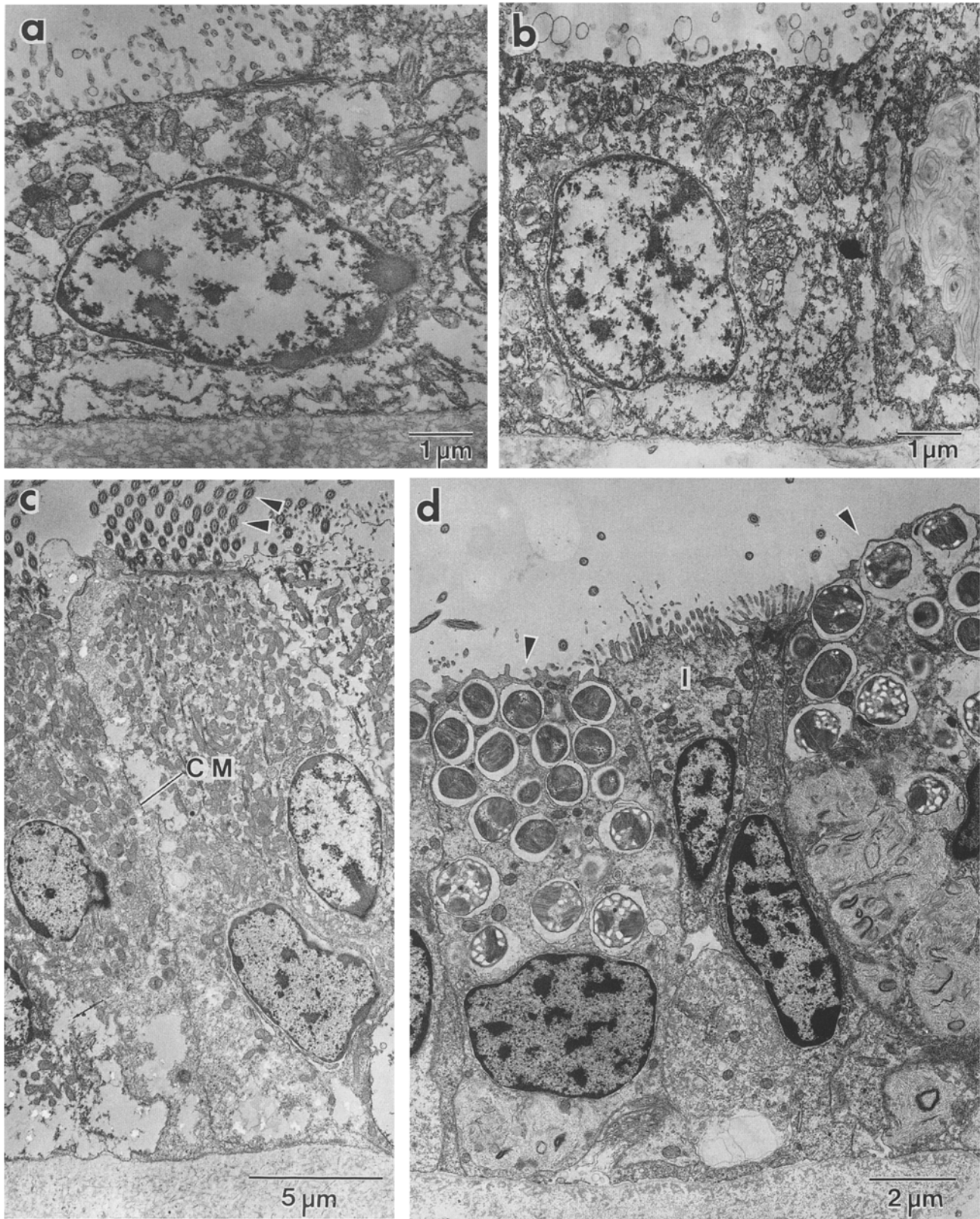


Fig. 4. *Bathymodiolus* sp. Electron micrographs of methane mussel gills. (a, b) Cross-sections through functionally aposymbiotic mussel gill-filaments; note lack of symbiont-containing vacuoles. (c) Cross-section through ciliated region of same aposymbiotic mussel gill-filament, showing quality of histological preservation; note pre-

servation of cilia (arrowheads) and cell membrane (CM). (d) Cross-section of freshly-collected methane-mussel gill-filament, showing a ciliated intercalary cell (I), flanked by symbiont-containing bacteriocyte cells (arrowheads)

Stoichiometric relationships between dissolved gas fluxes in whole mussels

The first series of respiration experiments was designed to examine stoichiometric relationships between rates of oxygen consumption, methane consumption, and carbon dioxide production in the intact symbiosis under a wide range of oxygen and methane conditions. Table 2 contains a summary of these results, all of which are based on gas chromatographic analyses.

The mussels in these experiments exhibited some variability in maximal rates of oxygen and methane consumption. Mussel 5, for example, consumed oxygen and methane at high rates (12.78 and 9.23 $\mu\text{mol g}^{-1} \text{h}^{-1}$, respectively). Mussels 9 and 11, on the other hand, consumed oxygen and methane at much lower maximal rates (3.35 and 1.79 $\mu\text{mol g}^{-1} \text{h}^{-1}$, and 2.99 and 1.43 $\mu\text{mol g}^{-1} \text{h}^{-1}$, respectively). These differences are most likely due to individual variation among the mussels in symbiont complement.

Analysis of covariance (ANCOVA) on the slopes of the linear regressions relating fluxes (O_2 consumption vs CH_4 consumption and CO_2 production vs CH_4 consumption) for individual mussels showed that variations between individuals were not significant ($p=0.1175$ and 0.6981 , respectively). It should be noted that there was a

high degree of "within regression variation" among these data, making it difficult to detect differences between regressions. However, this variation arises primarily from the limited sample size of some of the individual mussel data sets (Table 2), rather than from large-scale variation among the mussels.

The combined data set, taken from Experimental Mussels 1–11 inclusive, shows the following relationships in metabolic gas flux: The rate of oxygen consumption was significantly correlated with the rate of methane consumption, where: O_2 consumption ($\mu\text{mol g}^{-1} \text{h}^{-1}$) = $0.95 + 1.19 (\pm 0.09) \text{CH}_4$ consumption ($\mu\text{mol g}^{-1} \text{h}^{-1}$); $r^2=0.85$, $p<0.0001$). Similarly, the rate of carbon dioxide production was significantly correlated with the rate of methane consumption, where: CO_2 production ($\mu\text{mol g}^{-1} \text{h}^{-1}$) = $0.89 + 0.31 (\pm 0.06) \text{CH}_4$ consumption ($\mu\text{mol g}^{-1} \text{h}^{-1}$); $r^2=0.47$, $p<0.0001$; Fig. 5). Thus, per mol CH_4 consumed, the mussels consumed ~ 1.2 mol O_2 , and produced ~ 0.3 mol CO_2 . The y -axis intercepts of these regression lines show that around $0.89 \mu\text{mol CO}_2 \text{ g}^{-1} \text{h}^{-1}$ were produced per $0.95 \mu\text{mol O}_2 \text{ g}^{-1} \text{h}^{-1}$ consumed in the absence of CH_4 , yielding an estimated RQ of 0.94 for the mussel in the absence of methane consumption.

Stoichiometric relationships between dissolved gas fluxes in symbiont preparations

In these experiments, based on incubations in ^{14}C -labelled methane, the rates of $^{14}\text{CO}_2$ production were significantly correlated with total rates of $^{14}\text{CH}_4$ consumption (^{14}C remaining in tissues + $^{14}\text{CO}_2$ produced). The relationship between methane consumption and carbon dioxide production was, for S1: $^{14}\text{CO}_2$ production (nmol 10^{-8} cells h^{-1}) = $0.01 + 0.38 (\pm 0.05) ^{14}\text{CH}_4$ consumption (nmol 10^{-8} cells h^{-1}); $r^2=0.85$, $p<0.0001$); for S2: $^{14}\text{CO}_2$ production (nmol 10^{-8} cells h^{-1}) = $0.01 + 0.28 (\pm 0.02) ^{14}\text{CH}_4$ consumption (nmol 10^{-8} cells h^{-1}); $r^2=0.95$, $p<0.0001$; Fig. 6). In these preparations, stoi-

Table 1. *Bathymodiolus* sp. Results of bacterial counts of DAPI-stained gill homogenates from a freshly-collected mussel, a mussel maintained in captivity for 26 d, and a functionally aposymbiotic mussel. Duplicate homogenates were prepared and counted for each individual

Mussel	Bacteria/g gill tissue	SD
Freshly-collected	5.6×10^9	1.7×10^9
26 d post-capture	3.1×10^9	6.7×10^8
Aposymbiotic	6.1×10^8	4.2×10^8

Table 2. *Bathymodiolus* sp. Summary of experimental conditions and results of whole-mussel respiration experiments utilizing gas chromatographic analysis. Linear regression coefficients and r -squared values are underlined if not significant ($p<0.05$). Mussels

Mussel No.	wet wt	(n)	Gas concentrations (μM)		Maximal fluxes		Linear regression coefficients					
			$[\text{O}_2]$	$[\text{CH}_4]$	O_2	CH_4	$\text{O}_2 = a \text{CH}_4 + b$			$\text{CO}_2 = a \text{CH}_4 + b$		
							a	b	r^2	a	b	r^2
1	25.57	(10)	18–223	0–38	4.46	2.69	1.19	0.97	0.95	0.73	0.15	0.64
2	22.95	(12)	75–230	0–73	4.64	2.99	1.28	0.52	0.78	0.57	0.46	0.53
3	30.89	(13)	61–343	91–622	5.79	4.63	1.23	0.19	0.96	0.34	0.32	0.78
4	25.46	(13)	74–533	118–887	6.09	4.00	1.33	0.19	0.92	0.32	0.55	0.49
5	25.65	(17)	18–390	1–490	12.78	9.23	1.24	1.15	0.97	0.31	1.01	0.58
6	24.12	(9)	80–776	27–630	6.38	4.73	1.32	0.46	0.98	0.32	0.68	0.78
7	21.22	(16)	165–932	0–538	7.10	5.69	0.97	0.94	0.76	0.20	1.02	0.31
8	18.37	(17)	239–978	0–628	6.70	3.13	1.11	1.85	0.46	0.34	1.19	0.23
9	25.20	(4)	222–309	139–208	3.35	1.79	1.16	1.30	0.96	0.85	0.43	0.55
10	17.13	(6)	200–241	134–551	6.72	4.28	0.61	3.75	0.96	0.17	1.87	0.61
11	16.48	(6)	257–345	538–554	2.99	1.43	1.65	0.60	0.84	0.63	0.57	0.47

numbered according to order in which they were run; wet wt is shell-free wet tissue wt (g); (n): total number of measurements from which slope was calculated; O_2 , CH_4 , CO_2 : fluxes ($\mu\text{mol g}^{-1} \text{h}^{-1}$)

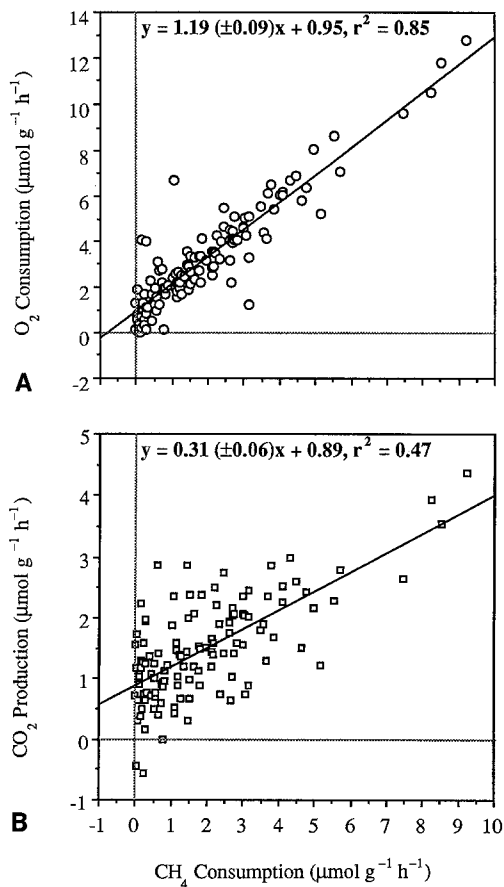


Fig. 5. *Bathymodiolus* sp. Combined GC data set (Mussels 1–11) showing stoichiometric relationships between oxygen consumption and methane consumption (A), and between carbon dioxide production and methane consumption (B) in mussels with functional symbionts. Consumption and production rates are expressed as $\mu\text{mol g (shell-free wet tissue wt)}^{-1} \text{h}^{-1}$. Slope of linear regressions expressed as slope $\pm 95\%$ confidence interval

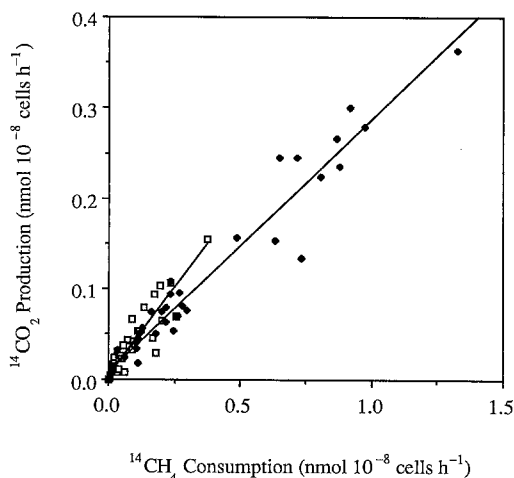


Fig. 6. *Bathymodiolus* sp. Results of bacterial preparation experiments, showing stoichiometric relationships between $^{14}\text{CO}_2$ production and total $^{14}\text{CH}_4$ consumption ($^{14}\text{CO}_2$ produced + ^{14}C incorporated) by symbiont preparations from two separate mussels (S1 and S2). Rates are expressed as $\text{nmol } 10^{-8} \text{ bacterial cells h}^{-1}$. Equations of linear regressions are: for S1 (\square), $y = 0.38 (\pm 0.05) x + 0.01$, $r^2 = 0.85$; for S2 (\blacklozenge), $y = 0.28 (\pm 0.02) x + 0.01$, $r^2 = 0.95$. Slopes are expressed $\pm 95\%$ confidence intervals

chiometric relationships between methane consumption and carbon dioxide production were similar to those found in whole mussels, with approximately one-third of the methane consumed being completely oxidized to CO_2 .

Effects of oxygen and methane concentrations on dissolved gas fluxes

The effects of oxygen and methane concentrations upon consumption rates by whole mussels were examined by two different approaches: (1) In portions of those experiments (Mussels 1–11) during which the mussels were exposed to a wide range of concentrations of one gas and a narrow range of the other, it was possible to examine the relationships between gas concentrations and production or consumption rates in extant data sets. In addition, we carried out experiments which made use of MIMS to measure gas concentrations and consumption or production rates, specifically designed to further elucidate these concentration effects. The use of MIMS increased sampling rates by an order of magnitude, allowing us to study the effects of changes in gas concentrations much more efficiently.

Oxygen concentration effects

Effects of oxygen limitation upon oxygen and methane consumption rates by an intact mussel were studied using MIMS to measure gas concentrations. In this experiment, oxygen concentrations were varied from 13 to $300 \mu\text{M}$ and methane concentrations were maintained between 100 and $400 \mu\text{M}$. Maximal rates of oxygen and methane consumption appear to occur at or above $300 \mu\text{M}$. At concentrations up to at least $300 \mu\text{M}$ O_2 , oxygen and methane consumption rates were dependent upon oxygen concentration. The mussels were apparently unable to consume oxygen to concentrations below $13 \mu\text{M}$ (Fig. 7). In experiments where oxygen was increased to much higher concentrations (Mussels 7 and 8), oxygen and methane consumption declined sharply above $500 \mu\text{M}$ O_2 . However, this inhibition persisted only until oxygen concentrations were returned to levels below $500 \mu\text{M}$.

Experiments were undertaken to determine whether the observed oxygen-dependency effects were of host or symbiont origin. Two whole-mussel experiments, both of which utilized the GC for dissolved gas analysis, were carried out on functionally aposymbiotic mussels. In these experiments, oxygen and methane consumption rates were measured over a wide range of oxygen concentrations with methane concentrations maintained between 150 and $200 \mu\text{M}$ CH_4 . Under these conditions oxygen consumption was found to be dependent upon oxygen concentration, increasing as a function of concentration up to 150– $250 \mu\text{M}$ O_2 , and decreasing at concentrations above this level (Fig. 8). This pattern is similar to that exhibited by mussels with intact symbionts, although in the functionally aposymbiotic individuals maximal

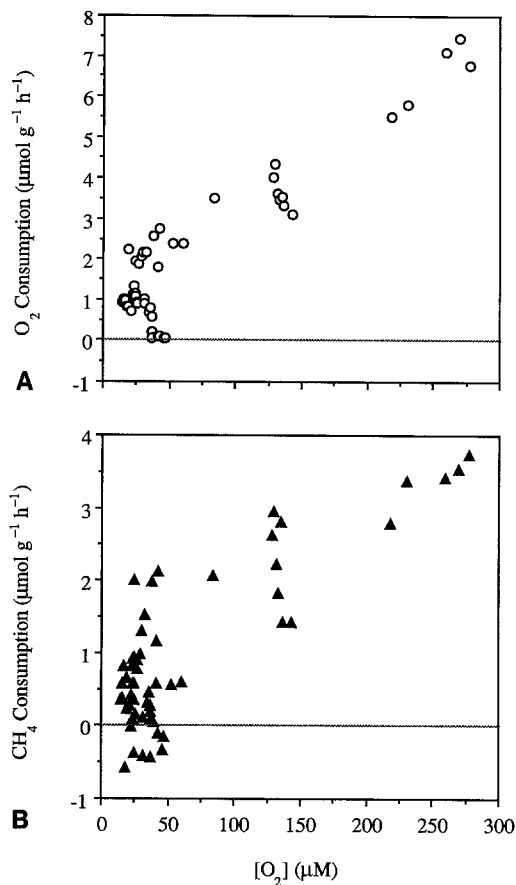


Fig. 7. *Bathymodiolus* sp. MIMS data, showing effects of oxygen concentration (*x*-axes) upon oxygen consumption (A) and methane consumption (B) by a whole mussel with intact symbionts. Methane concentrations ranged from 100 to 400 μM. “Production” of oxygen and methane (negative consumption) represents error in rate measurements. Note different scales on *y*-axes

oxygen consumption rates were below 1 μmol O₂ g⁻¹ h⁻¹ vs a maximum value of 8 μmol O₂ g⁻¹ h⁻¹ by a mussel with functional symbionts incubated in the presence of methane (Fig. 7).

Methane concentration effects

Experiments similar to those described above were used to examine effects of methane concentration on oxygen and methane consumption rates in symbiont-containing and functionally aposymbiotic mussels. In two of the whole-mussel GC experiments (Mussels 5 and 8), methane concentrations were gradually decreased while oxygen concentrations were maintained in the range 120 to 390 μM (Fig. 9). Below 250 μM CH₄, oxygen and methane consumption rates declined as a function of methane concentration. Given adequate oxygen, the mussels were capable of consuming methane to concentrations below the level of reliable detectability (~5 μM), showing that although methane consumption is dependent upon concentration up to high methane concentrations, the mussels are capable of taking it up at very low external levels.

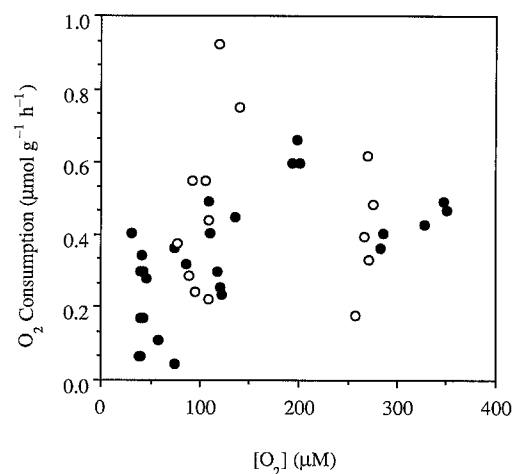


Fig. 8. *Bathymodiolus* sp. GC data, showing effects of oxygen concentration on rates of oxygen consumption by two functionally aposymbiotic mussels. Methane concentrations ranged from 150 to 200 μM

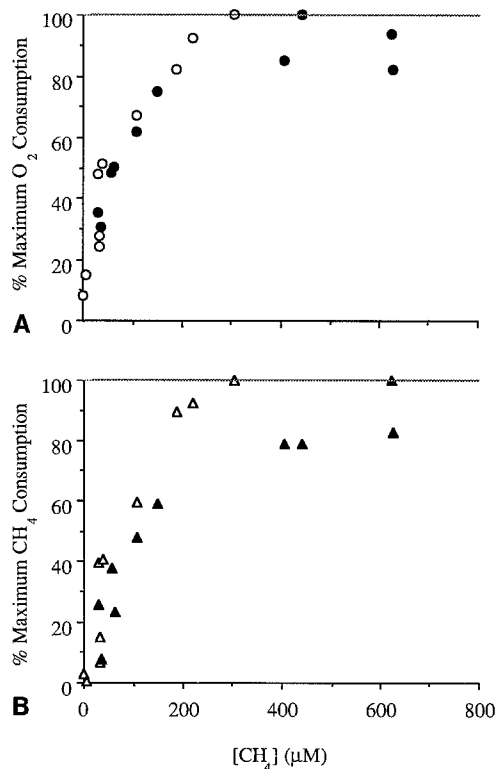


Fig. 9. *Bathymodiolus* sp. GC data showing effects of limiting methane concentrations on maximal rates of oxygen consumption (A) and methane consumption (B) by Mussels 5 (○, △) and 8 (●, ▲). Maximal rates of oxygen and methane consumption were 12.8 and 6.7 μmol g⁻¹ h⁻¹ and 9.2 and 3.1 μmol g⁻¹ h⁻¹ for Mussels 5 and 8, respectively. Oxygen concentrations ranged from 120 to 390 μM

Maximal oxygen and methane consumption rates occurred at methane concentrations > 250 μM, with maximum rates of 9.23 and 3.13 μmol CH₄ g⁻¹ h⁻¹ and 12.78 and 6.70 μmol O₂ g⁻¹ h⁻¹ for Mussels 5 and 8, respectively.

In a separate MIMS experiment where oxygen and methane consumption rates were measured across a wide

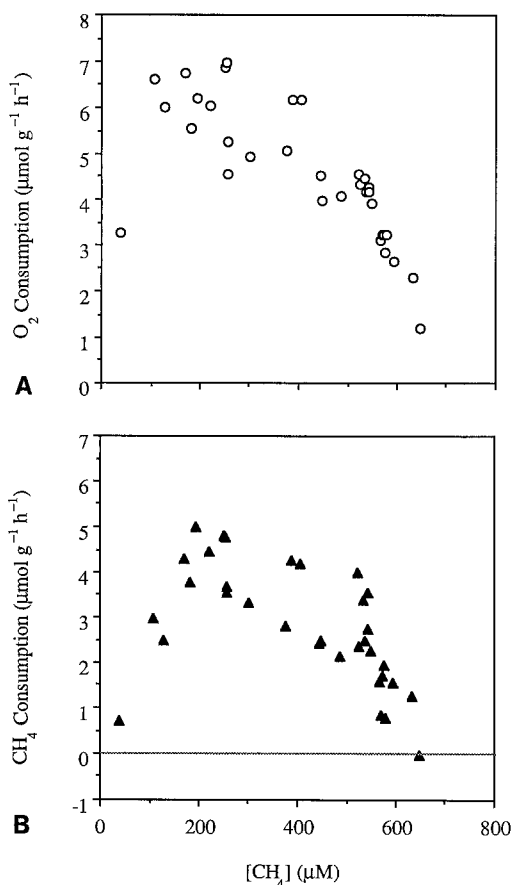


Fig. 10. *Bathymodiolus* sp. MIMS data showing effects of high methane concentrations on rates oxygen consumption (A) and methane consumption (B) by a mussel with functional symbionts. Oxygen concentrations ranged from 100 to 400 μM

range of methane concentrations, with oxygen concentrations between 100 and 400 μM O₂, maximum oxygen and methane consumption occurred at methane concentrations in the range 150 to 350 μM CH₄, with a decrease in consumption above this range. This pattern is demonstrated in Fig. 10, which shows that inhibition of oxygen and methane consumption began above 400 μM CH₄. Methane consumption was completely inhibited above 650 μM CH₄, and oxygen consumption declined to functionally aposymbiotic rates in this concentration range. Similar patterns of oxygen and methane consumption were exhibited by other mussels when exposed to similar conditions (Mussels 3, 4, 10, and 11).

Experiments were carried out on functionally aposymbiotic mussels to determine whether the observed methane concentration effects were of symbiont or host origin. Using the GC for dissolved gas analysis, oxygen and methane consumption rates by a functionally aposymbiotic mussel were measured over a wide range of methane concentrations (0 to 750 μM CH₄), with oxygen concentrations held fairly constant (150 to 300 μM O₂). Under all experimental conditions, oxygen consumption rates were constant, without depression at high methane concentrations, and methane consumption was negligible (Fig. 11). Similar results were obtained from three other functionally aposymbiotic mussels under similar condi-

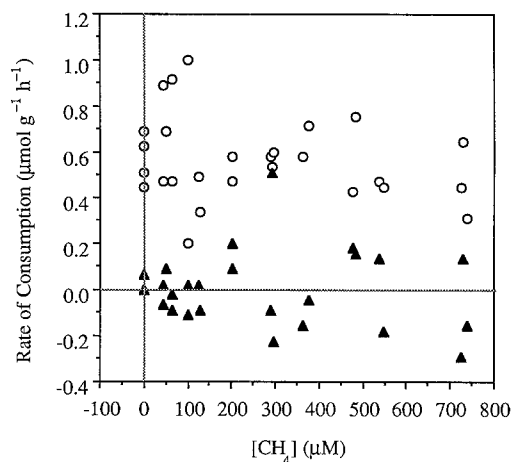


Fig. 11. *Bathymodiolus* sp. GC data showing effects of methane concentration on rates of oxygen consumption (○) and methane consumption (▲) by a functionally aposymbiotic mussel. Oxygen concentrations ranged from 150 to 300 μM. Note that methane “production” (negative consumption) represents error in rate measurements

tions, although none of these other individuals were exposed to such a wide range of methane concentrations. In all the experiments with functionally aposymbiotic mussels, rates of oxygen and methane consumption were much lower than those exhibited by mussels with functional symbionts.

Nitrogen consumption by methane mussels

Dissolved molecular nitrogen (N₂) concentrations and fluxes were monitored in all whole-mussel experiments. However, no significant rates of nitrogen consumption or production were detected under any of the conditions tested.

Discussion

The data presented here describe the functioning of one of the few symbioses described thus far in which the symbionts rely upon methane, rather than sulfide, as a source of chemical reducing power. Because methane is not toxic, and because it serves as the carbon source as well as the electron donor in this association, the methane mussels (*Bathymodiolus* sp.) offer a unique perspective upon the functioning of animal/invertebrate symbioses.

Electron microscopy and bacterial counts

The lack of methane consumption by those mussels exposed to warm water showed them to be functionally aposymbiotic; if symbionts were present, they did not exhibit detectable methanotrophic activity. TEM examination of sections from freshly-collected and functionally aposymbiotic mussel gills indicated a drastic reduction in symbiont numbers (Fig. 4). The few bodies present which

bore any similarity to the symbiotic bacteria normally present in bacteriocytes were amorphous and not readily identifiable as symbionts. Even the bacteriocytes themselves appeared to have degenerated, unlike the adjacent ciliated portions of gill tissue (Fig. 4b, c). Examination of DAPI-stained gill homogenates indicated a 90% reduction of appropriately sized, DAPI positive (DNA-containing) bodies in the functionally aposymbiotic mussel gills (Table 1). Furthermore, the DAPI-stained bodies in these gills were noticeably less regular in shape compared to the uniform spheres counted in homogenates of gills from a freshly-collected mussel. Thus, the available evidence suggests that these mussels were aposymbiotic in the strictest sense.

Stoichiometry

The methane mussels assimilate methane with high efficiency. Per mole of CH_4 consumed, mussels with functional symbionts produce ~ 0.3 mol CO_2 . This ratio indicates that the bacteria completely oxidize only a fraction of the methane they consume, with about 70% presumably being incorporated as organic compounds. Similar efficiency was found in isolated symbiont preparations, suggesting that it is an inherent symbiont characteristic.

The ratio of oxygen consumption to methane consumption in whole mussels was ~ 1.2 mol O_2 per mol CH_4 , which lies between the expected 1:1 ratio for partial oxidation of methane for biosynthesis (to CH_2O), and the 1:2 ratio expected for complete oxidation of CH_4 to CO_2 . This suggests that 80% of the methane consumed is incorporated by the symbiosis, which agrees well with the value of 70% calculated above.

Estimates of carbon conversion efficiency (% of substrate carbon converted to cell material) for free-living Type I methanotrophs range from 38 to 63%, depending upon the specific hydroxylation pathway utilized (Anthony 1982). Thus, our values of 70 to 80% places the mussels' symbionts at the high end of the efficiency scale, attesting to the overall efficiency of the functioning symbiosis.

Oxygen consumption

Oxygen demand generated by bacterial methane oxidation leads to extraordinarily high overall rates of oxygen consumption in the intact association. The highest rates we measured were > 12 $\mu\text{mol O}_2 \text{ g}^{-1} \text{ h}^{-1}$, and typical consumption rates were in the range 6 to 7 $\mu\text{mol O}_2 \text{ g}^{-1} \text{ h}^{-1}$ (Table 2). If converted to units of $\text{ml O}_2 \text{ g dry wt}^{-1} \text{ h}^{-1}$ (assuming dry wt = 18.5% wet wt, based on measurements of *Bathymodiolus thermophilus*: Fisher et al. 1988), typical rates ranged from 0.73 to 0.85 $\text{ml O}_2 \text{ g dry wt}^{-1} \text{ h}^{-1}$, with the highest rate measured (12.78 $\mu\text{mol O}_2 \text{ g}^{-1} \text{ h}^{-1}$) equal to about 1.55 $\text{ml O}_2 \text{ g dry wt}^{-1} \text{ h}^{-1}$. These rates are ~ 4 to 5 times those measured in other, non-symbiotic species of mussels at similar temperatures (Bayne 1976).

In the absence of methane, mussels with functional symbionts exhibited rates of oxygen consumption between 1.0 and 1.5 $\mu\text{mol O}_2 \text{ g}^{-1} \text{ h}^{-1}$. If these rates are converted as above, they come to 0.12–0.18 $\text{ml O}_2 \text{ g dry wt}^{-1} \text{ h}^{-1}$, which are more typical of rates measured in other mytilids at similar temperatures (Bayne 1976). In functionally aposymbiotic mussels rates were slightly lower, ranging from 0.6 to 1.0 $\mu\text{mol O}_2 \text{ g}^{-1} \text{ h}^{-1}$. This difference is probably due to the decrease in organic carbon (food) available to the host, leading to a general decline in metabolic rate. The aposymbiotic condition is akin to starvation in heterotrophic mussels, and indeed the metabolic rates of these individuals agreed well with those measured in other species after a period of starvation (Bayne 1976).

Differences in maximal rates of oxygen consumption exhibited by symbiont-containing mussels exposed to methane, symbiont-containing mussels without methane, and functionally aposymbiotic mussels show that there is very high bacterial demand for oxygen during methane oxidation. The extent of this demand may be illustrated by calculating the change in oxygen consumption in symbiont-containing mussel gills exposed to methane: a mussel with functional symbionts, in the absence of methane, consumes ~ 1 $\mu\text{mol O}_2 \text{ g}^{-1} \text{ h}^{-1}$, of which $\sim 30\%$ (0.3 $\mu\text{mol g}^{-1} \text{ h}^{-1}$) may be attributed to the gills, based on percentage of total wet weight (Page et al. 1990). Maximal rates of oxygen consumption by mussels with functional symbionts in the presence of methane range from 3.0 to 12.8 $\mu\text{mol g}^{-1} \text{ h}^{-1}$, with a median value of 6 $\mu\text{mol g}^{-1} \text{ h}^{-1}$ (Table 2). Since this increase (5 $\mu\text{mol g}^{-1} \text{ h}^{-1}$) arises in the gills, it actually reflects an increase of 16.7 $\mu\text{mol g}(\text{gill tissue})^{-1} \text{ h}^{-1}$. Thus, bacterial methane oxidation generates an oxygen demand over 50 times higher in symbiont-containing gill tissue than in gills of individuals not exposed to methane.

The response of the methane mussel symbiosis to reduced environmental oxygen tensions is typical of mytilid bivalves. From maximal rates measured at oxygen concentrations near saturation, oxygen consumption declines as a function of decreasing oxygen concentration, to a minimum concentration below which no consumption is measured. In the intact symbiosis, maximal rates of oxygen consumption occur at oxygen concentrations near saturation, ~ 300 μM . This value agrees well with the findings of Cary et al. (1988), which showed maximal shell growth at an oxygen concentration of 290 $\mu\text{M O}_2$. Below 300 μM , consumption declines gradually with decreasing oxygen concentration to around 50 μM , at which point it drops off sharply (Fig. 7A). The lowest concentration at which oxygen consumption was detectable was 13 $\mu\text{M O}_2$ (≈ 6.8 mm Hg), which agrees well with values reported for other mytilids (4 to 13 mm Hg; Mangum and Winkle 1973). Oxygen consumption in the intact association is a nearly linear function of oxygen concentration between 50 and 300 μM [O_2 consumption ($\mu\text{mol g}^{-1} \text{ h}^{-1}$) = $0.523 + 0.02x - 1.463 \cdot 10^{-5}x^2$, where $x = [\text{O}_2]$ (μM)]. The linearity of this regression indicates that in this range of concentrations the intact symbiosis has minimal regulatory capacity for oxygen (Mangum and Winkle 1973).

Functionally aposymbiotic mussels exhibit a similar response to reduced oxygen tensions, although maximal consumption rates occur at slightly lower oxygen partial pressures (150 to 250 μM ; Fig. 8). Below 200 μM O_2 , oxygen consumption declines in a manner similar to that exhibited by symbiont-containing mussels, with a polynomial regression of: O_2 consumption ($\mu\text{mol g}^{-1} \text{h}^{-1}$) = $0.101 + 2.717 \cdot 10^{-3} x + 8.128 \cdot 10^{-7} x^2$. Once again, the near linearity of this function suggests that little oxygen uptake regulation occurs in the host mussels.

The similarity of response patterns between symbiotic and functionally aposymbiotic mussels to reduced oxygen tensions shows that the bacterial endosymbionts play little part in the regulation of gas exchange by the intact association. Studies on free-living methanotrophs have measured bacterial K_m s for oxygen in the range of 0.4 to 11.1 μM (Hughes and Wimpenny 1969), well below levels of apparent oxygen limitation exhibited by the intact symbiosis. Thus, although they dramatically increase the overall oxygen demand, the symbionts apparently rely upon the host ventilatory mechanisms for oxygen uptake and are subject to the limits of its effectiveness. Compared to the elaborate gas-transport schemes exhibited by other deep-sea animal/bacterial associations (e.g. *Riftia pachyptila*, Arp and Childress 1983, Childress et al. 1984, Arp et al. 1985; *Calyptogena magnifica*, Arp et al. 1984, Childress et al. 1991), this is somewhat restrictive, as it apparently limits the association's metabolism at low oxygen concentrations. Given the relatively high ambient oxygen concentrations in the seep environment, however, it is unlikely that such restrictions play a significant role in the functioning of the symbiosis in situ.

Methane consumption

When methane mussels are incubated with adequate concentrations of oxygen, they are capable of consuming methane at extremely high rates, to very low concentrations. The dependence of consumption rate upon concentration (Fig. 9B) suggests that methane uptake, like oxygen uptake, is dependent upon host ventilation mechanisms. Previous studies which measured oxygen and methane consumption and carbon dioxide production by excised mussel gills showed similar substrate concentration effects, with all three declining as oxygen and methane were depleted from the incubation medium (Childress et al. 1986).

In this symbiosis, methane uptake has been measured at methane concentrations below the limits of reliable detectability ($\sim 5 \mu\text{M}$ CH_4), suggesting high bacterial methane affinity. Studies utilizing different techniques have shown some free-living methanotrophs to have K_m values for methane as low as 0.8 to 2.0 μM CH_4 , and suggest that K_m values around 1 μM CH_4 are probably typical of these bacteria (Joergensen and Degn 1983). Thus, as with oxygen, the high affinities of the symbionts as well as their physical location near the surface of the gill cells provide a sufficient methane supply to sustain very high rates of consumption. However, these rates are also subject to limitation at lower methane concentrations, apparently imposed by the host tissues.

When mussels with active symbionts are exposed to methane concentrations $> 300 \mu\text{M}$, there is a gradual decrease in rates of oxygen and methane consumption. A similar pattern was observed in shell growth experiments, in which the highest rates of shell growth were measured at 245 μM CH_4 , which was the lowest methane concentration tested (Cary et al. 1988; it should be noted that oxygen concentrations were decreased at higher methane concentrations in these experiments, allowing the possibility that the observed effect was due to oxygen limitation rather than methane inhibition). No such decline was exhibited by functionally aposymbiotic mussels incubated under these conditions, however, suggesting that this inhibition arises in the symbionts. One possible explanation for this phenomenon is that some intermediate product of methane oxidation is concentrated in the bacteria, eventually reaching inhibitory levels. (Both formaldehyde and formate are intermediate products in the oxidation of methane to carbon dioxide, either of which are potential toxins; Anthony 1982.) This assertion is supported by the apparent lack of inhibition exhibited by Mussel 8 at methane concentrations $> 300 \mu\text{M}$ (Fig. 9B). Because this mussel exhibited lower methane consumption rates, it would be less apt to form high concentrations of any putative inhibitory intermediate compounds such as formaldehyde or formate.

Whole-mussel model

Methane mussels apparently lack the high degree of specialization exhibited by other animal/bacterial symbioses. Because methane is not toxic, and because it does not spontaneously react with oxygen, these mussels are not confronted with many of the problems faced by their sulfide-oxidizing counterparts. Furthermore, because oxygen and methane are present simultaneously in the seep communities, they do not require elaborate chemical transport and storage mechanisms to utilize their energy source.

Despite their lack of obvious specialization, this symbiosis has shown the highest potential net carbon incorporation rate of any animal/bacterial symbiosis studied thus far. The highest rate of methane consumption measured in a methane mussel ($9.23 \mu\text{mol g}^{-1} \text{h}^{-1}$) corresponds to a net carbon incorporation rate (CH_4 consumption $-\text{CO}_2$ production) of nearly $5 \mu\text{mol g}^{-1} \text{h}^{-1}$. More typical maximal carbon incorporation rates exhibited by several other methane mussels were in the range of 2.3 to 4.0 $\mu\text{mol g}^{-1} \text{h}^{-1}$. To compare, the highest rate of net CO_2 incorporation by the sewage clam *Solemya reidi* was $0.89 \mu\text{mol g}^{-1} \text{h}^{-1}$ (Anderson et al. 1987). In *Riftia pachyptila*, the giant vestimentiferan tubeworm of the hydrothermal vents, it was $\sim 2 \mu\text{mol g}^{-1} \text{h}^{-1}$ (Childress et al. 1991).

A useful way to evaluate this rate of carbon incorporation is in terms of the potential for growth it provides. For a mussel with a wet weight of 25 g, $\sim 8.7\%$ (2.2 g) will be carbon (based upon chemical composition measurements of *Bathymodiolus thermophilus*; Fisher et al. 1988). From this, and assuming no other nutrient limita-

tions, for a given rate of methane consumption and carbon dioxide production it is possible to predict the growth rate of the mussel. For example, a net carbon uptake of $5 \mu\text{mol g}^{-1} \text{h}^{-1}$ yields a rate of increase in organic carbon of 1.6%/d. More typical rates of carbon uptake (2.3 to $4.0 \mu\text{mol g}^{-1} \text{h}^{-1}$) correspond to rates in the range 0.77 to 1.33%/d. These rates are much higher than those of *Solemya reidi* (0.24%/d), and are comparable to those of *Riftia pachyptila* (1.4%/d; Childress et al. 1991).

Although these calculations are founded upon actual measurements of respiration rates, the high degree of respiratory dependence exhibited for oxygen and methane by this symbiosis suggest that in situ rates are highly dependent upon environmental concentrations of these dissolved gases. Using our data, it is possible to construct a model for rates of growth under conditions which may exist in situ. The first step is to determine the relationship between methane concentration and consumption. This can be approximated by a polynomial regression of the data in Fig. 9B, which relates methane consumption (% maximum) to methane concentration. Because methane concentrations above $\sim 300 \mu\text{M}$ were found to be inhibiting to mussels with high methane consumption rates, and because concentrations in this range have not been measured in the seep environment, the model will only concern concentrations in the range 0 to $300 \mu\text{M CH}_4$. The resulting equation is: % max. CH_4 consumption = $-0.001x^2 + 0.545x + 0.726$, where $x = [\text{CH}_4]$ (μM). In this model, the use of "% max. CH_4 consumption" is necessitated by the variability in rates among the two mussels upon which it is based.

Using this equation it is possible to calculate rates of methane consumption across the range of concentrations from 0 to $300 \mu\text{M CH}_4$, based upon a given maximum rate of methane consumption. With this, calculations of growth are readily accomplished. Fig. 12 shows a series of curves, each of which is based upon a different maximum rate of methane consumption. The lowest curve,

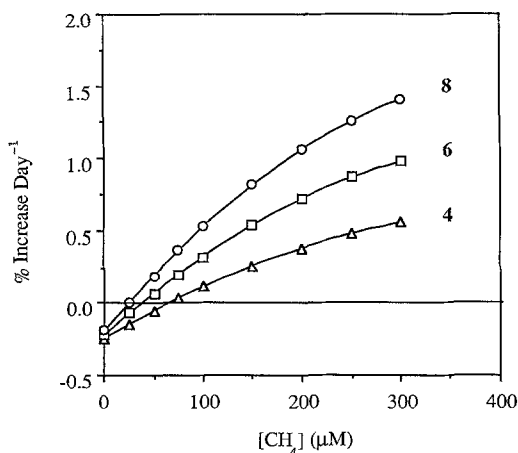


Fig. 12. *Bathymodiolus* sp. Effect of methane concentration upon net rate of carbon assimilation (expressed as % increase), predicted by model using maximal methane consumption rates of 4 and $\mu\text{mol g}^{-1} \text{h}^{-1}$ (Δ), $6 \mu\text{mol g}^{-1} \text{h}^{-1}$ (\square), and $8 \mu\text{mol g}^{-1} \text{h}^{-1}$ (\circ), for a 25 g mussel with a carbon content of 8.65% wet weight

based on a maximum rate of $4 \mu\text{mol g}^{-1} \text{h}^{-1}$, shows the mussel to be capable of net growth at methane concentrations $> 60 \mu\text{M CH}_4$. The highest curve, based on a maximum rate of $8 \mu\text{mol g}^{-1} \text{h}^{-1}$, shows net carbon uptake around $25 \mu\text{M CH}_4$, with a growth rate of $\sim 0.5\%/d$ at $100 \mu\text{M CH}_4$.

Data concerning the environmental chemistry in the seeps are scarce. Analyses of bulk water samples taken in the immediate vicinity of the mussels show methane concentrations to be moderate, on the order of 60 to $70 \mu\text{M}$ maximum (MacDonald et al. 1989). Oxygen concentrations are much higher (150 to $200 \mu\text{M O}_2$; I. MacDonald personal communication), and thus probably need not be considered as a limiting factor in growth-rate calculations. Maximal methane uptake rates of freshly-collected mussels are typically between 4 and $5 \mu\text{mol g}^{-1} \text{h}^{-1}$. Based on these values, calculated rates of growth with methane as the sole carbon source range up to 0.1%/d. This rate is only $\sim 10\%$ of that measured in *Riftia pachyptila*, and less than half that measured in *Solemya reidi*. However, it clearly shows that net carbon uptake from endosymbiotic methane utilization is possible within the seep habitat.

Conclusions

Bivalves harboring bacterial endosymbionts are widespread in the deep sea. The success of these types of associations is apparent when we consider the wide range of geographic locations and habitat types in which they dominate. Several species of bivalves have been studied which contain bacteria capable of utilizing reduced sulfur compounds as a source of energy (Fisher 1990). The methane mussels are similar to these other deep-sea symbioses, in that they lack obvious specializations, other than enlarged gills where their symbionts are housed. However, their ability to utilize methane as a source of energy and carbon distinguishes them from the majority of the deep-sea symbioses described thus far.

From the data presented here, we see that neither the methane mussels nor their bacterial endosymbionts display remarkable characteristics not found in their free-living counterparts. The mussels do not appear to have evolved any special mechanisms for concentrating or transporting metabolic gases, and thus like other mytilids their metabolic rates are profoundly dependent upon environmental concentrations of respiratory gases. The bacteria apparently have high affinities for oxygen and methane, as do free-living methanotrophs. While the hosts support dense populations of symbionts in their gills, they also limit the metabolic rates which these symbionts can achieve due to the poor regulatory abilities imposed by the mytilid body plan and physiology. Thus, the success of this symbiosis may not result so much from specialization as from the general versatility and physiological suitability of the symbiotic partners.

Note

Work in progress has shown that within the seep habitat, methane mussels may normally be exposed to concentra-

tions of methane in the range from 150 to 200 μM , much higher than previously supposed. Additionally, it appears that methane consumption rates on the order of 10 to 13 $\mu\text{mol g}^{-1} \text{h}^{-1}$ may be typical of freshly collected mussels. These observations suggest that, in situ, the methane mussels may be capable of achieving substantial carbon assimilation rates, in excess of 2% per day, solely through symbiotic methane fixation.

Acknowledgements. The authors would like to thank the captains and crews of the R. V. "Seaward Explorer" and the R. V. "Edwin C. Link", as well as the submarine pilots and crews of the "Pisces II" and the "Johnson Sea Link I". We would like to thank R. W. Lee, E. V. Thuesen, L. A. Gorodezky, and D. R. Oros for their technical assistance and for critically reviewing this manuscript, as well as J. A. Favuzzi, J. M. Zande, N. I. Shapiro, and R. N. Fariss for providing technical support. Finally we thank our reviewers, who made many helpful suggestions. This work was supported by ONR Grant N00014-88-K-0177 to CRF and JJC.

Literature cited

- Anderson, A. E., Childress, J. J., Favuzzi, J. (1987). Net uptake of CO_2 driven by sulfide and thiosulfate oxidation in the bacterial symbiont-containing clam *Solemya reidi*. *J. exp. Biol.* 133: 1–31
- Anthony, C. (1982). *The biochemistry of methylotrophs*. Academic Press, London
- Arp, A. J., Childress, J. J. (1981). Blood function in the hydrothermal vent vestimentiferan tube worm. *Science*, N.Y. 213: 342–344
- Arp, A. J., Childress, J. J. (1983). Sulfide binding by the blood of the hydrothermal vent tube worm *Riftia pachyptila*. *Science*, N.Y. 219: 295–297
- Arp, A. J., Childress, J. J., Fisher, C. R., Jr. (1984). Metabolic and blood gas transport characteristics of the hydrothermal vent bivalve, *Calyptogena magnifica*. *Physiol. Zoöl.* 57: 648–662
- Arp, A. J., Childress, J. J., Fisher, C. R., Jr. (1985). Blood gas transport in *Riftia pachyptila*. *Bull. Biol. Soc. Wash.* 6: 289–300
- Bayne, B. L. (1976). *Marine mussels, their ecology and physiology*. Cambridge University Press, Cambridge
- Brooks, J. M., Kennicutt, M. C., II, Fisher, C. R., Macko, S. A., Cole, K., Childress, J. J., Bidigare, R. R., Vetter, R. D. (1987). Deep-sea hydrocarbon seep communities: evidence for energy and nutritional carbon sources. *Science*, N.Y. 238: 1138–1142
- Cary, S. C., Fisher, C. R., Felbeck, H. (1988). Mussel growth supported by methane as sole carbon and energy source. *Science*, N.Y. 240: 78–80
- Cavanaugh, C. M., Gardiner, S. L., Jones, M. L., Jannasch, H. W., Waterbury, J. B. (1981). Prokaryotic cells in the hydrothermal vent tube worm *Riftia pachyptila*: possible chemoautotrophic symbionts. *Science*, N.Y. 213: 340–342
- Childress, J. J., Arp, A. J., Fisher, C. R., Jr. (1984). Metabolic and blood characteristics of the hydrothermal vent tube-worm *Riftia pachyptila*. *Mar. Biol.* 83: 109–124
- Childress, J. J., Fisher, C. R., Brooks, J. M., Kennicutt, M. C., II, Bidigare, R., Anderson, A. (1986). A methanotrophic marine molluscan symbiosis: mussels fueled by gas. *Science*, N.Y. 233: 1306–1308
- Childress, J. J., Fisher, C. R., Favuzzi, J. A., Kochevar, R. E., Sanders, N. K., Alayse, A. M. (1991). Sulfide-driven autotrophic balance in the bacterial symbiont-containing hydrothermal vent tubeworm, *Riftia pachyptila* Jones. *Bull. mar. biol. Lab.*, Woods Hole 180: 135–153
- Distel, D. L., Felbeck, H. (1988). Pathways of inorganic carbon fixation in the endosymbiont bearing lucinid clam *Lucinoma aequizonata*: Part 2. Analysis of the individual contributions of host and symbiont to inorganic carbon assimilation. *J. exp. Zool.* 247: 11–22
- Felbeck, H., Somero, G. N., Childress, J. J. (1981). Calvin-Benson cycle sulphide oxidation enzymes in animals from sulphide rich habitats. *Nature*, Lond. 293: 291–293
- Fisher, C. R. (1990). Chemoautotrophic and methanotrophic symbioses in marine invertebrates. *CRC critical. Rev. aquat. Sciences* 2: 399–436
- Fisher, C. R., Childress, J. J., Arp, A. J., Brooks, J. M., Distel, D., Favuzzi, J. A., Felbeck, H., Hessler, R., Johnson, K. S., Kennicutt, M. C., II, Macko, S. A., Newton, A., Powell, M. A., Somero, G. N., Soto, T. (1988). Microhabitat variation in the hydrothermal vent mussel *Bathymodiolus thermophilus*, at Rose Garden vent on the Galapagos rift. *Deep-Sea Res.* 35: 1769–1792
- Fisher, C. R., Childress, J. J., Oremland, R. S., Bidigare, R. R. (1987). The importance of methane and thiosulfate in the metabolism of the bacterial symbionts of two deep-sea mussels. *Mar. Biol.* 96: 59–71
- Heinzle, E., Furukawa, K., Dunn, I. J., Bourne, J. R. (1983). Experimental methods for on-line mass spectrometry in fermentation technology. *Biotechnology* 1(2): 181–188
- Hobbie, J. E., Daley, R. J., Jasper, S. (1977). Use of Nuclepore filters for counting bacteria by fluorescence microscopy. *Appl. envirl Microbiol.* 33: 1225–1228
- Hughes, D. E., Wimpenny, J. W. T. (1969). Oxygen metabolism by microorganisms. *Adv. microb. Physiol.* 3: 197–232
- Joergensen, L., Degn, H. (1983). Mass spectrometric measurements of methane and oxygen utilization by methanotrophic bacteria. *Fedn eur. microbiol. Soc. (FEMS) Lett.* 20: 331–335
- MacDonald, I. R., Boland, G. S., Baker, J. S., Brooks, J. M., Kennicutt, M. C., II, Bidigare, R. R. (1989). Gulf of Mexico hydrocarbon seep communities. II. Spatial distribution of seep organisms and hydrocarbons at Bush Hill. *Mar. Biol.* 101: 235–247
- Mangum, C., Winkle, W. V. (1973). Responses of aquatic invertebrates to declining oxygen conditions. *Am. Zool.* 13: 529–541
- Muller, L. L., Jacks, T. J. (1975). Rapid chemical dehydration of samples for electron microscopic examinations. *J. Histochem. Cytochem.* 23: 107–110
- Page, H. M., Fisher, C. R., Childress, J. J. (1990). Role of filter-feeding in the nutritional biology of a deep-sea mussel with methanotrophic symbionts. *Mar. Biol.* 104: 251–257
- Schmaljohann, R., Flügel, H. J. (1987). Methane-oxidizing bacteria in Pogonophora. *Sarsia* 72: 91–98
- Somero, G. N., Anderson, A. E., Childress, J. J. (1989). Transport, metabolism and detoxification of hydrogen sulfide in animals from sulfide rich marine environments. *CRC critical Rev. aquat. Sciences* 1: 591–614